Nanoparticles

DOI: 10.1002/ange.200906835

A Seed-Based Diffusion Route to Monodisperse Intermetallic CuAu Nanocrystals**

*Wei Chen, Rong Yu, Lingling Li, Annan Wang, Qing Peng, and Yadong Li**

Because of their size- and composition-dependent properties,[1–5] the controlled synthesis of metal nanocrystals (NCs) with tunable sizes and compositions is of great significance for understanding and exploring their properties, as well as for their use in novel materials. As a class of particular metal materials, intermetallic compounds often exhibit better physical and chemical properties than the constituent metals and corresponding disordered alloys, for example, highly efficient catalytic performance,[6–8] magnetism,[9] and excellent structural stability at high temperatures,[10] which arise from their various compositions and ordered crystal structures. Particularly, intermetallic noble–nonnoble NCs may be the ideal candidates of new low-cost catalysts with desired performance.[6,8]

In the past two decades, much progress has been achieved on the controlled synthesis of single-metal nanocrystals.[3,4,11–18] However, fabrication of monodisperse NCs of intermetallic compounds with tunable sizes is more difficult and limited strategies have been developed. Traditional methods such as the high-temperature melting technique and ball milling make only bulk materials.[19] Annealing disordered alloys directly may lead to corresponding ordered intermetallics,[9,20] and some other steps are necessary to avoid sintering for redispersion of the NCs in solvents.[20] Schaak and co-workers have reported two typical routes: 1) co-reduction of ionic metal precursors and subsequent annealing in an inert gas or a high-boiling-point solvent,[21,22] and 2) chemical conversion from metal nanocrystals.[23–25] The size distribution of the products still need some improvement. Nonhydrolytic colloidal synthesis may be powerful, but it is difficult to realize simultaneous reduction of different metal ions and to choose suitable capping agents.[26–29] Accordingly, the controlled synthesis of intermetallics NCs is still a great challenge and more efforts are required for exploring their new properties and applications.

Herein, taking the CuAu system as a typical example, we report a protocol employing the diffusion of newly produced Cu atoms into presynthesized Au NCs to prepare monodisperse intermetallic CuAu NCs, as described in Equation (1). With this method, the size and monodispersity of the sample could be fine-tuned based on those of the Au nanoparticles precursor. Additionally, selective synthesis of CuAu and Cu_3Au could also be realized readily by changing the molar ratio of the starting materials.

$$Au + Cu^{2+} + OA/TOA \xrightarrow{\Delta} Cu_3Au \text{ or } CuAu \quad (1)$$

The synthesis according to Equation (1) was typically conducted by heating a mixture of $Cu(CH_3COO)_2$, presynthesized Au nanoparticles (stoichiometric amount), oleic acid (OA), and tri-*n*-octylamine (TOA) at an appropriate temperature for 50–100 min and then cooling to room temperature. The product could be well dispersed in a nonpolar organic solvent such as hexane. As reported previously, galvanic replacement reactions [Eq. (2)] are

$$3\,Ag + Au^{3+} \rightarrow 3\,Ag^{+} + Au \quad (2)$$

usually employed to obtain nanostructures of alloys and lower-activity metals.[11,30,31] Each of those reactions requires a metal precursor with a lower reduction potential. The difference of redox potentials between two metals promotes the reaction. It is notable that in our system [Eq. (1)], NCs of Au, whose reduction potential is higher than metallic Cu, were used as the precursor. In this case, examples of epitaxial growth were reported.[32,33] With our method, we have produced intermetallic CuAu NCs. The powder X-ray diffraction (XRD) patterns (Figure 1) of the Cu_3Au and CuAu products made at different temperatures by using 6.3 nm and 8.5–9.5 nm Au seeds, respectively (see Figure S1 in the Supporting Information), reveal that intermetallic Cu_3Au formed at 300 °C when the Cu/Au atomic ratio was set as 3:1. All the reflections of the sample can be assigned to cubic ordered Cu_3Au (JCPDS 35-1357). When equimolar amounts of raw material were used, intermetallic CuAu was obtained at 280 °C (JCPDS 65-2798). Superlattice reflections of *001* and *110,* and the splitting reflections of *200/002* and *220/202* are clearly visible. In the synthesis, a stoichiometric amount of reagents is important for getting the corresponding intermetallic sample. If $Cu(CH_3COO)_2$ and Au with molar ratio of 2:1 were used, the XRD data (Figure S3 in the Supporting Information) reveal that the final product contained zero-valent Cu and an unknown specimen, which may be a phase

[*] W. Chen, L. L. Li, A. N. Wang, Dr. Q. Peng, Prof. Y. D. Li
Department of Chemistry and
State Key Laboratory of New Ceramics and Fine Processing
Tsinghua University, Beijing 100084 (China)
Fax: (+86) 10-6278-8765
E-mail: ydli@mail.tsinghua.edu.cn
ydli@mail.tsinghua.edu.cn
Dr. R. Yu
State Key Laboratory of New Ceramics and Fine Processing
Department of Materials Science and Engineering
Tsinghua University, Beijing 100084 (China)

[**] We thank Prof. J. Zhu from Beijing National Center for Electron Microscopy for help in TEM characterization. This work was supported by the NSFC (20921001, 90606006) and the State Key Project of Fundamental Research (2006CB932300).

Supporting information for this article is available on the WWW under http://dx.doi.org/10.1002/anie.200906835.

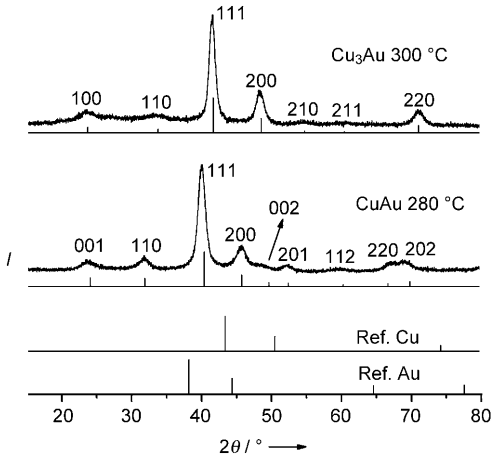

Figure 1. XRD patterns of (from bottom to top) reference Cu; reference Au; reference intermetallic CuAu; as-prepared intermetallic CuAu from 8.5–9.5 nm Au NCs at 280 °C; reference intermetallic Cu_3Au; and as-prepared Cu_3Au from 6.3 nm Au NCs at 300 °C.

between CuAu and Cu_3Au.

Figure 2 a,b exhibits the transmission electron microscopy (TEM) images of the as-obtained (10.0 ± 0.3) nm Cu_3Au and (11.0 ± 0.6) nm CuAu NCs. The NCs are spherical and have narrow size distributions. The size distribution histograms (Figure S2 in the Supporting Information) further confirm the size uniformity. The NCs inherit the monodispersity of the Au NCs precursor (Figure S1). Figure 2 c,d presents typical high-resolution TEM (HRTEM) photographs of corresponding Cu_3Au and CuAu NCs, respectively. The obvious boundaries on the surface of the particles reveal that the spherical particles have polyhedral shape. The pseudo-fivefold axis further indicates that the NCs have pseudo-icosahedral or -decahedral topologies, which arise from that of Au (Figure S4). If searched for carefully, single-crystal-like particles (not ideal single crystals, Figure S5) could be found which maybe grew from single-crystalline Au NCs (Figure S4). Most of the Au nanoparticles (< 10 nm) are multiply twinned particles with polyhedral morphology for minimizing energy and a few are the single crystals.[34,35] Accordingly, most of the intermetallic CuAu NCs have multiply twinned structures. However, the insertion of Cu atoms may destroy the ideal icosahedral or decahedral topology, especially for the product with a higher Cu/Au atomic ratio (Cu_3Au). Figure 2 e,f gives the electron diffraction patterns of the as-prepared Cu_3Au and CuAu NCs, which agree well with the XRD data (Figure 1). All the reflections can be assigned to intermetallic cubic Cu_3Au and tetragonal CuAu crystalline structure. Notably, the characteristic superlattice reflections of *001* and *110*, and splitting reflections of *200/002* and *220/202* of CuAu were observed. Although the *001* and *110* reflections of ordered Cu_3Au also appear, their signal was not intense, which is consistent with its XRD pattern (Figure 1) in which the *001* and *110* peaks have relative lower intensity. The energy-dispersive X-ray spectra (EDS) (Figure S6) show the elements of Cu and Au in the products (Mo and Ni were from the grids) and give Cu/Au atomic ratios of 73:27 and 52:48, respectively, which are in agreement with the compositions of Cu_3Au and tetragonal CuAu within the error range. The EDS results of a single nanoparticle (Figure S7) further confirm the stoichiometric compositions of the products.

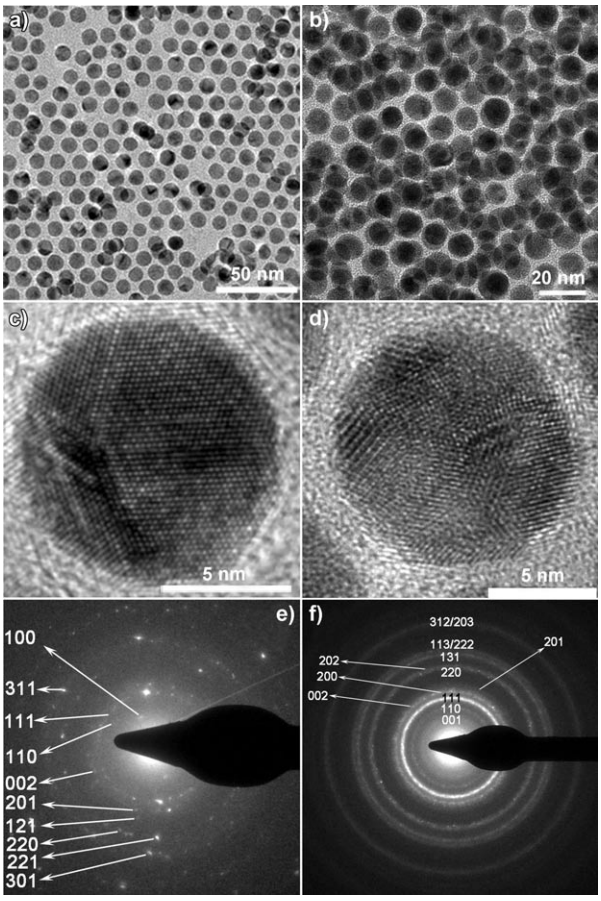

Figure 2. TEM, HRTEM images, and selected-area electron diffraction patterns of a,c,e) Cu_3Au from 6.3 nm Au NCs and b,d,f) CuAu from 8.5–9.5 nm Au NCs.

To check that the synthetic method we designed is powerful in controlling the size of intermetallic NCs, pre-synthesized Au NCs with different sizes were used for the synthesis. Taking the preparations of intermetallic CuAu at 280 °C as examples, the XRD patterns in Figure S8 (Supporting Information) indicate that when 3.5 and 4.9 nm Au NCs were used as seeds, only disordered CuAu (alloy) was produced after 50 min. When the system was heated for 100 min, the appearance of superlattice reflections (*001* and *110*) implies the formation of intermetallic CuAu. If larger Au particles (6.3 nm or 8.5–9.5 nm) were employed as the precursors, the production of ordered CuAu needed only 50 min (Figure S8 e, Figure 1). Actually, ordering of smaller particles was harder to achieve because of the higher strain force. Figure 3 a–c lists the TEM images of the as-synthesized ordered CuAu NCs with different sizes, indicating that all the samples contain monodisperse nanoparticles. The size distribution histograms also reveal the size monodispersity (Figure S9). The size of the NCs is quite dependent on that of the Au seeds, and analysis of TEM micrographs revealed that CuAu NCs with sizes of (4.2 ± 0.2), (6.0 ± 0.2), and (7.4 ± 0.3) nm resulted from Au NPs with sizes of 3.5, 4.9, and

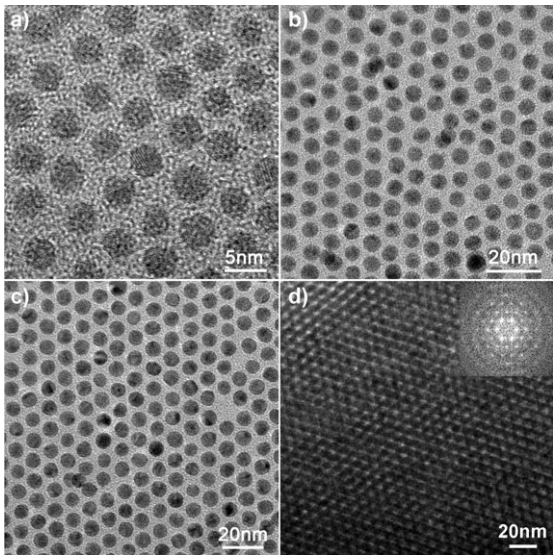

Figure 3. TEM images of the intermetallic CuAu with different sizes: a) (4.2 ± 0.2) nm, b) (6.0 ± 0.2) nm, c) (7.4 ± 0.3) nm; d) TEM image of a multilayer hcp superlattice consisting of (6.0 ± 0.2) nm CuAu NCs; inset shows the corresponding fast Fourier transform (FFT) pattern.

6.3 nm (Figure S1),[36] respectively. Therefore, it is easy to realize size-control with this protocol. The narrow size distribution enabled the as-synthesized CuAu NCs to form three-dimensional (3D) superlattices by self-assembly. Figure 3d depicts the TEM image of a typical superlattice of 6.0 nm CuAu NCs assembled on a carbon-coated copper grid after steady evaporation of the organic solvent. The TEM image and corresponding fast Fourier-transform (FFT) pattern (inset) both indicate a 3D superlattice beautifully aligned with the hexagonal closed-packed (hcp) structure. For clarity, Figure S10 shows the TEM image of a superlattice consisting of only two layers of NCs, which formed when the concentration of the colloidal solution was decreased.

From the above results, we can deduce a diffusion-based mechanism similar to that of a solid-state reaction for the formation of intermetallic CuAu (Figure 4). In our synthesis system, capping molecules on the surface of Au seeds had a higher probability to desorb and then escape into the solution because of the temperature used, leaving active sites on the Au surface. Because of the synergetic effect of TOA/OA and Au NCs,[37] Cu^{2+} ions were reduced to Cu atoms or clusters with high activity.[38] Meanwhile, the newly produced highly reactive Cu atoms or clusters collided with the active sites of Au particles and diffused from the surface into the crystal lattice of Au seeds to form a CuAu solid solution (alloy) because of the thermal energy. The formation of the alloy would induce reduction on Au surface[37] and make the reduction and diffusion reactions proceed simultaneously. The elevated temperature supplied enough thermal energy for the ordering and finally produced the intermetallic NCs.

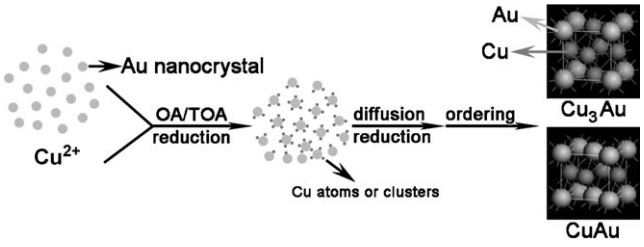

Figure 4. Proposed mechanism for the formation of the intermetallic NCs.

To ensure the rationality of the mechanism, aliquots at different stages were taken out from the system for characterization and analysis (taking the reaction preparing intermetallic CuAu with 4.9 nm Au seeds as the example, the Cu/Au ratio of the reagents was 1:1). Figure S11 (Supporting Information) presents the visible absorption spectra of the products obtained after different lengths of time, which were employed to monitor the conversion process. The absorption spectrum of the sample taken when the temperature reached 180 °C (at a heating rate of 25 °C min^{-1}) supplies at least two pieces of information: 1) the absence of a maximum peak in the spectrum and red-shifting of the dominating absorption edge (about 528 nm) relative to the absorption peak of Au seeds ($\lambda_{abs} = 514$ nm) indicate the insertion of Cu atoms; 2) the absence of an absorption peak of Cu NCs implies that the newly reduced Cu atoms diffused quickly into the Au seeds and that the diffusion rate was faster than the formation of zero-valent Cu, and thus no Cu NCs exists in the obtained product. The light greenish color of the mother solution after centrifugation further showed that reduction and diffusion had not proceeded to completion. In fact, the TEM image (Figure 5a) shows that the sample in this case contained monodisperse nanoparticles with size of 5.4 nm, which were larger than the Au seeds (4.9 nm) owing to the insertion of Cu atoms. The uniformity of the NCs and absence of any irregular particles directly reveals that no amorphous Cu or Cu NCs stayed in the product. The corresponding EDS analysis (Figure 5b) gives a Cu/Au atomic ratio of about 27:73, namely, 37.0% of Cu had diffused into the Au lattice.

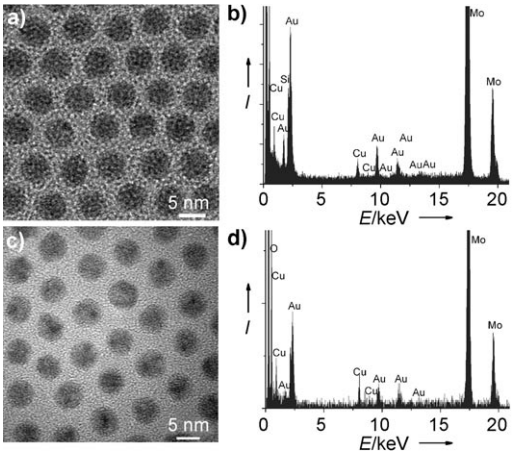

Figure 5. TEM images and EDS spectra of the products at different stages: a,b) when the temperature reached 180 °C, showing ca. 5.4 nm particles and an Cu/Au atomic ratio of 27:73; c,d) when the temperature was increased to 190 °C, showing ca. 6.0 nm NCs and a Cu/Au atomic ratio of 45:55.

When the system was heated to 190 °C, the dominating absorption edge further red-shifted to about 550 nm and showed no obvious change as the temperature was further increased, showing that the diffusion of Cu atoms almost finished by 190 °C. Actually, the colorless mother solution after separation also reveals the approximate end of the reduction and diffusion. From then on, the heating and aging served mainly for ordering. The TEM photograph (Figure 5c) reveals that the NCs at 190 °C grew to approximately 6.0 nm, which is as large as the final intermetallic CuAu NCs. A Cu/Au atomic ratio of nearly 1:1 (considering the error) obtained from the EDS spectrum (Figure 5d) also implies that diffusion was almost completed. Provided that the increase of the size resulted completely from the entering of Cu atoms and the particles were ideal spheres, then the percentage of the Cu that had diffused into Au at 180 °C could be calculated as $(5.4^3-4.9^3)/(6.0^3-4.9^3)\times 100\,\%$ (about 40.5 %), which was approximately consistent with the EDX result (37.0 %) as described above.

If the reaction was conducted without Au NCs at 180 °C for 30 min, only a little Cu (< 5 %, dispersed in hexane) was obtained. Even when the system was kept at 190 °C for 50 min, less than 10 % of Cu^{2+} was reduced. The red purple solution of as-produced Cu NCs in hexane quickly changed to green in air, indicating the oxidation of Cu to Cu_2O.[38] These results reveal that without Au, the equilibrium constants of the reaction (reduction of Cu^{2+} to Cu) at 180 and 190 °C were too small. The formation of CuAu alloy would destroy the equilibrium and then accelerate the reduction process.[37]

Because the intermetallic and alloyed CuAu NCs have nearly the same absorption (Figure S11 in the Supporting Information), the absorption spectrum cannot offer the information of ordering. For this purpose, XRD data at different stages were collected to show the ordering. As shown in Figure S12, by 180 and 190 °C, no reflections of Cu could be found and the peaks shifted to higher angle region relative to those of Au, confirming the diffusion of Cu atoms. As the temperature was continuously increased after reaching 190 °C, the (111) peak slightly moved and the superlattice signals appeared after aging at 280 °C for 100 min, displaying the ordering process. Accordingly, the formation of Cu atoms and their diffusion were quite fast, whereas the ordering was the rate-limiting step during the whole synthesis.

The diffusion of Cu atoms in the reaction with Cu/Au ratio of 2:1 was similar to that with Cu/Au ratio of 1:1 except that the complete diffusion needs a higher temperature (250 °C) (Figures S13 and S14). Furthermore, the ordering cannot produce a pure intermetallic compound (Figure S3).

All the experimental results and analysis listed above support the given mechanism. In fact, the hypothesis for our designed reaction is a modified solid-state reaction. The reagents of a typical solid-state reaction are often solid powders, which are irregular particles and cannot be completely mixed together. Thus, it is difficult for a solid-state reaction to realize homogeneous diffusion and then to produce monodisperse NCs. In our protocol, the reaction occurred between uniformly dispersed Au nanoparticles and the in situ reduced active Cu atoms or clusters in solution. The homogeneous collision, atomic-scale diffusion, and ordering in solution, together with the monodisperse Au particle templates, jointly led to the intermetallic NCs with narrow size distributions.

In summary, a seed-based diffusion route using Au NCs as precursors was developed to fabricate monodisperse intermetallic CuAu and Cu_3Au NCs, which had great advantages in controlling the size and monodispersity. The results indicated that the diffusion of newly produced active Cu atoms into Au lattice and subsequent ordering might be the main process for the formation intermetallic nanocrystals. This methodology provides a clue that "moving" a solid-state reaction into solution may allow homogeneous diffusion and need less time and thermal energy but produce monodisperse NCs. Our recent advances showed that it is useful for synthesizing other important intermetallic or alloyed NCs such as Cu_xPd_{1-x} and Cu_xPt_{1-x} (Figure S15), which is helpful for scientists to exploit low-cost catalysts and other useful materials urgently required for scientific and technical applications.

Experimental Section

Synthesis of intermetallic CuAu nanocrystals (NCs): First, Au nanoparticle (NP) precursors were prepared with the previously reported procedure[36] with some modifications. For the synthesis of intermetallic CuAu NCs, $Cu(CH_3COO)_2{\cdot}H_2O$ (0.5 mmol), oleic acid (OA; 0.5 mL), and tri-*n*-octylamine (TOA; 2.25 mL) were mixed together in a flask and heated to 70 °C to form a clear solution, into which the as-prepared Au NPs solution was injected. When hexane completely evaporated, the temperature was raised to 120 °C under Ar flow to remove water. After about 20 min, the solution was heated to 280 °C at a rate of around 25 °C min^{-1} and kept for 50–100 min before it was cooled to room temperature. If the Cu/Au atomic ratio was set as 3:1 and the mixture was kept at 300 °C, ordered Cu_3Au could be obtained. The product was collected by ethanol addition, subsequent centrifugation, and finally dispersion into 20 mL hexane.

Characterization: The phase of the product was determined by a Rigaku D/max 2500Pc X-ray powder diffractometer with $Cu_{K\alpha}$ radiation ($\lambda = 1.5418$ Å), and the sample was dropped on a amorphous glass. TEM, HRTEM images, and EDX spectra were recorded on a JEOL JEM-1200EX transmission electron microscope and FEI Tecnai G2 F20 S-Twin working at 200 kV. The adsorption spectra were obtained on a Hitachi U-3010 UV/Vis spectrometer.

Received: December 4, 2009
Published online: March 15, 2010

Keywords: alloys · copper · diffusion · gold · nanoparticles

[1] N. D. Spencer, R. C. Schoonmaker, G. A. Somorjai, *Nature* **1981**, *294*, 643 – 644.
[2] M. Valden, X. Lai, D. W. Goodman, *Science* **1998**, *281*, 1647 – 1650.
[3] V. F. Puntes, K. M. Krishnan, A. P. Alivisatos, *Science* **2001**, *291*, 2115 – 2117.
[4] N. Tian, Z.-Y. Zhou, S.-G. Sun, Y. Ding, Z. L. Wang, *Science* **2007**, *316*, 732 – 735.
[5] B. Lim, M. Jiang, P. H. C. Camargo, E. C. Cho, J. Tao, X. Lu, Y. Zhu, Y. Xia, *Science* **2009**, *324*, 1302 – 1305.
[6] A. Elattar, T. Takeshita, W. E. Wallace, R. S. Craig, *Science* **1977**, *196*, 1093 – 1094.
[7] C. Roychowdhury, F. Matsumoto, V. B. Zeldovich, S. C. Warren, P. F. Mutolo, M. Ballesteros, U. Wiesner, H. D. Abruna, F. J. DiSalvo, *Chem. Mater.* **2006**, *18*, 3365 – 3372.

[8] H. Abe, F. Matsumoto, L. R. Alden, S. C. Warren, H. D. Abruña, F. J. DiSalvo, *J. Am. Chem. Soc.* **2008**, *130*, 5452 – 5458.
[9] S. Sun, C. B. Murray, D. Weller, L. Folks, A. Moser, *Science* **2000**, *287*, 1989 – 1992.
[10] A. I. Taub, R. L. Fleischer, *Science* **1989**, *243*, 616 – 621.
[11] Y. Sun, Y. Xia, *Science* **2002**, *298*, 2176 – 2179.
[12] F. Kim, S. Connor, H. Song, T. Kuykendall, P. Yang, *Angew. Chem.* **2004**, *116*, 3759 – 3763; *Angew. Chem. Int. Ed.* **2004**, *43*, 3673 – 3677.
[13] Y. Yin, C. Erdonmez, S. Aloni, A. P. Alivisatos, *J. Am. Chem. Soc.* **2006**, *128*, 12671 – 12673.
[14] T. K. Sau, C. J. Murphy, *J. Am. Chem. Soc.* **2004**, *126*, 8648.
[15] C. Li, K. L. Shuford, Q.-H. Park, W. Cai, Y. Li, E. J. Lee, O. C. Cho, *Angew. Chem.* **2007**, *119*, 3328; *Angew. Chem. Int. Ed.* **2007**, *46*, 3264.
[16] W. Niu, S. Zheng, D. Wang, X. Liu, H. Li, S. Han, J. Chen, Z. Tang, G. Xu, *J. Am. Chem. Soc.* **2009**, *131*, 697 – 703.
[17] X. Huang, S. Tang, H. Zhang, Z. Zhou, N. Zheng, *J. Am. Chem. Soc.* **2009**, *131*, 13916 – 13917.
[18] Q. Zhang, Ge, T, Pham, Goebl, Y. X. Hu, Z. Lu, Y. Yin, *Angew. Chem.* **2009**, *121*, 3568 – 3571; *Angew. Chem. Int. Ed.* **2009**, *48*, 3516 – 3519.
[19] C. Suryanarayana, E. Ivanov, V. V. Boldyrev, *Mater. Sci. Eng. A* **2001**, *304–306*, 151 – 158.
[20] J. Kim, C. Rong, J. P. Liu, S. Sun, *Adv. Mater.* **2009**, *21*, 906 – 909.
[21] A. K. Sra, R. E. Schaak, *J. Am. Chem. Soc.* **2004**, *126*, 6667 – 6672.
[22] B. M. Leonard, N. S. P. Bhuvanesh, R. E. Schaak, *J. Am. Chem. Soc.* **2005**, *127*, 7326 – 7327.
[23] N. H. Chou, R. E. Schaak, *J. Am. Chem. Soc.* **2007**, *129*, 7339 – 7345.
[24] R. E. Cable, R. E. Schaak, *J. Am. Chem. Soc.* **2006**, *128*, 9588 – 9589.
[25] M. E. Anderson, M. R. Buck, I. T. Sines, K. D. Oyler, R. E. Schaak, *J. Am. Chem. Soc.* **2008**, *130*, 14042 – 14043.
[26] S. Maksimuk, S. Yang, Z. Peng, H. Yang, *J. Am. Chem. Soc.* **2007**, *129*, 8684 – 8685.
[27] S. Sun, *Adv. Mater.* **2006**, *18*, 393 – 403.
[28] D. Xu, Z. Liu, H. Yang, Q. Liu, J. Zhang, J. Fang, S. Zou, K. Sun, *Angew. Chem.* **2009**, *121*, 4281 – 4285; *Angew. Chem. Int. Ed.* **2009**, *48*, 4217 – 4221.
[29] J. Zhang, J. Fang, *J. Am. Chem. Soc.* **2009**, *131*, 18543 – 18547.
[30] S. E. Skrabalak, J. Chen, Y. Sun, X. Lu, L. Au, C. M. Cobley, Y. Xia, *Acc. Chem. Res.* **2008**, *41*, 1587 – 1595.
[31] Y. Sun, C. Lei, *Angew. Chem.* **2009**, *121*, 6956 – 6959; *Angew. Chem. Int. Ed.* **2009**, *48*, 6824 – 6827.
[32] S. E. Habas, H. Lee, Radmilovic, G. A. Somorjai, P. . Yang, *Nat. Mater.* **2007**, *6*, 692 – 697.
[33] J. Zhang, Y. Tang, L. Weng, M. Ouyang, *Nano Lett.* **2009**, *9*, 4061 – 4065.
[34] Z. L. Wang, *J. Phys. Chem. B* **2000**, *104*, 1153 – 1175.
[35] F. Baletto, R. Ferrando, *Phys. Rev. B* **2001**, *63*, 155408.
[36] S. Peng, Y. Lee, C. Wang, H. Yin, S. Dai, S. Sun, *Nano Res.* **2008**, *1*, 229.
[37] H. Jiang, K. Moon, C. P. Wong, *IEEE Trans. Adv. Packag.* **2005**, 173 – 177.
[38] M. Yin, C. Wu, Y. Lou, C. Burda, J. T. Koberstein, Y. Zhu, S. O'Brien, *J. Am. Chem. Soc.* **2005**, *127*, 9506 – 9511.

